Optimisation of a Fabry-Pérot cavity and Final Focus for CERN ICS

Vlad Muşat

Supervisor: Andrea Latina

Contents

Inverse Compton Scattering (ICS)

ICS = Scattering of a low energy photon from a relativistic electron resulting in a high energy x-ray

- ICS first described by Feenberg and Primakoff in 1948 [1].
- Several existing ICS sources: **ThomX** (France), **TTX** (China), **MuCLS** (Germany), etc.
- Applications include cancer therapy [2], X-ray imaging [3], cultural heritage [4], protein crystallography [5] and nuclear waste management [6].

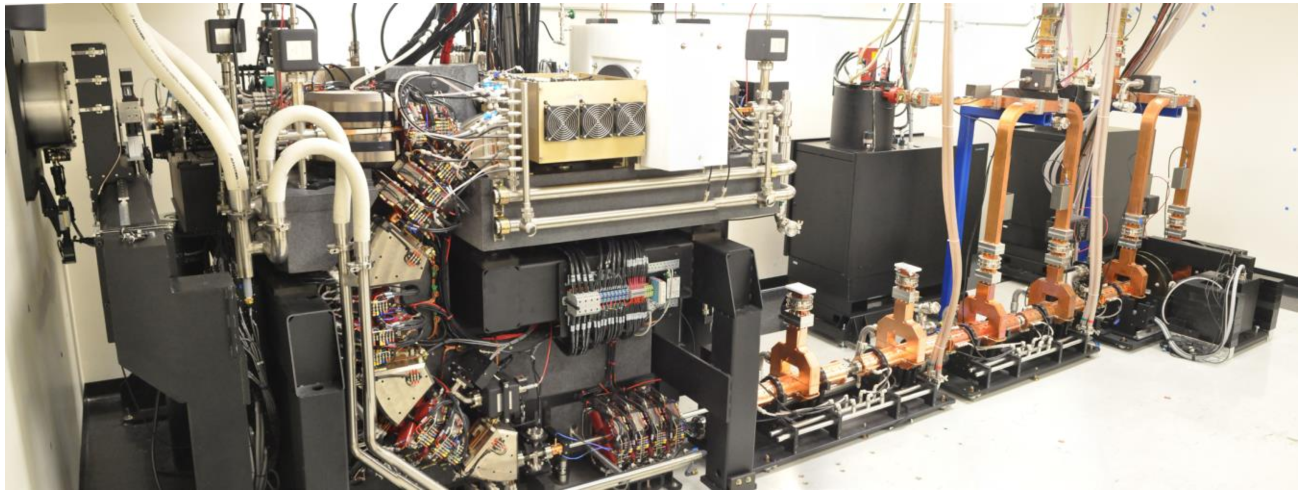

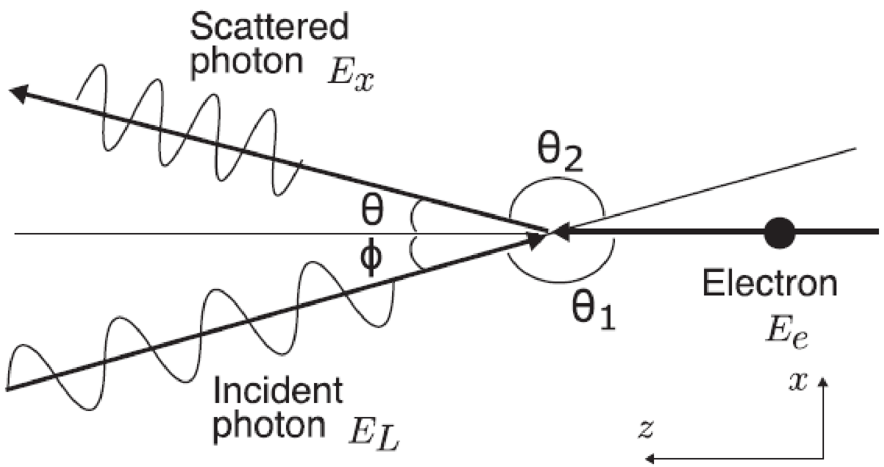

[1] Feenberg, E., & Primakoff, H. (March 01, 1948). Interaction of Cosmic-Ray Primaries with Sunlight and Starlight. Physical Review, 73, 5, 449-469.
[2] Montay-Gruel, P., et al. (December 01, 2018). X-rays can trigger the FLASH effect: Ultra-high dose-rate synchrotron light source prevents normal brain injury after whole brain irradiation in mice. Radiotherapy and Oncology, 129, 3, 582-588.
[3] Gradl, R., et al. (2017). Propagation-based Phase-Contrast X-ray Imaging at a Compact Light Source. (Scientific reports.)
[4] Walter, P., et al. (September 01, 2009). A new high quality X-ray source for Cultural Heritage. Comptes Rendus - Physique, 10, 7, 676-690.
[5] McCormick, et al. (January 01, 2010). X-ray structure determination of the glycine cleavage system protein H of Mycobacterium tuberculosis using an inverse Compton synchrotron X-ray source. *Journal of Structural and Functional Genomics, 11,* 1, 91-100
[6] Hajima, R., et al. (May 01, 2008). Proposal of Nondestructive Radionuclide Assay Using a High-Flux Gamma-Ray Source and Nuclear Resonance Fluorescence. Journal of Nuclear Science and Technology, 45, 5, 441-451.

Potential applications

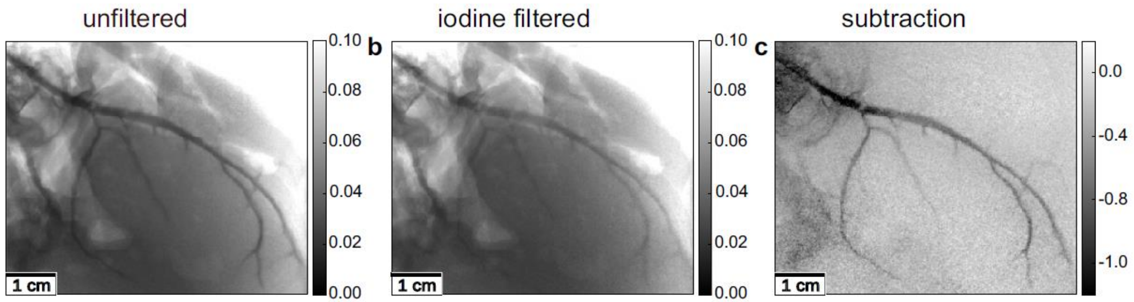

Ref: Kulpe, S., Dierolf, M., et al (December 10, 2018). K-edge subtraction imaging for coronary angiography with a compact synchrotron X-ray source. *Plos One, 13,* 12.)

- Many applications were a result of previous studies at synchrotrons. ICS sources offer a more compact and accessible method to conduct such experiments, and there is hope that in the near future such devices will also be implemented in hospitals or laboratories.
- The main challenge currently is achieving high intensity and high energy x-rays, similar to the ones in synchrotron sources.
- Tomographies in particular have already been extensively studied.

Name	E_{Xray} [keV]	$\mathcal{F}$ [ph/s]	BW [%]	σ_{Xray} (at IP) [μm]	σ_{Xray} (at sample) [mm]	Θ [mrad]
K-edge subtraction	33.7	3×10^{10}	4.5	6	16	4
Phase contrast imaging	25	2.4×10^{9}	4	39×45	16	4
Microbeam radiation therapy	25	10^{13}	3.6	70	4	1.5
FLASH therapy	6.000–10.000	10^{14}	-	50	17	-
Protein crystallography	7–35	10^{13}	1.4	30	30	2
XRF	6.5-92	3×10^{10}	1-3	20	20×10^{-3}	-
Nuclear waste management	1.000–5.000	2.2×10^{13}	0.2	35	-	-

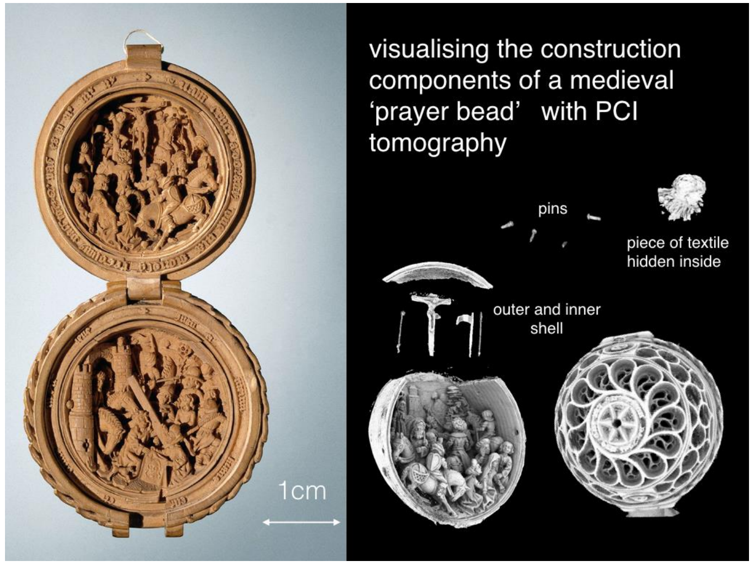

Ref: Reischig, P., et al (March 09, 2009). A note on medieval microfabrication: The visualization of a prayer nut by synchrotron-based computer X-ray tomography. *Journal of Synchrotron Radiation, 16,* 2, 310-313.

Landscape of ICS sources

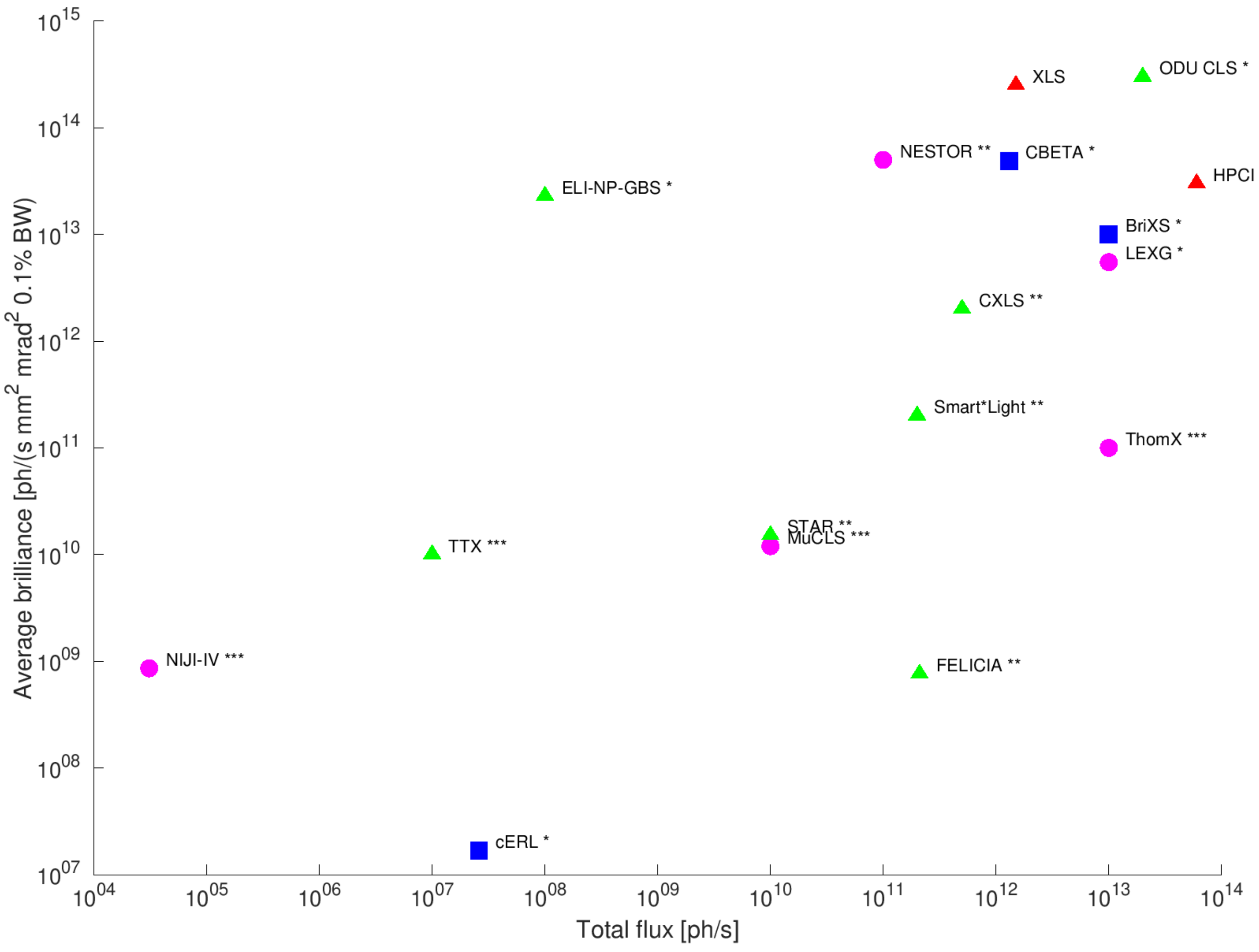

$$\mathcal{B} \approx \frac{\gamma^2 \mathcal{F}_{0.1\%}}{4\pi^2 \epsilon_x^N \epsilon_y^N}$$

RF-Track: Code benchmark

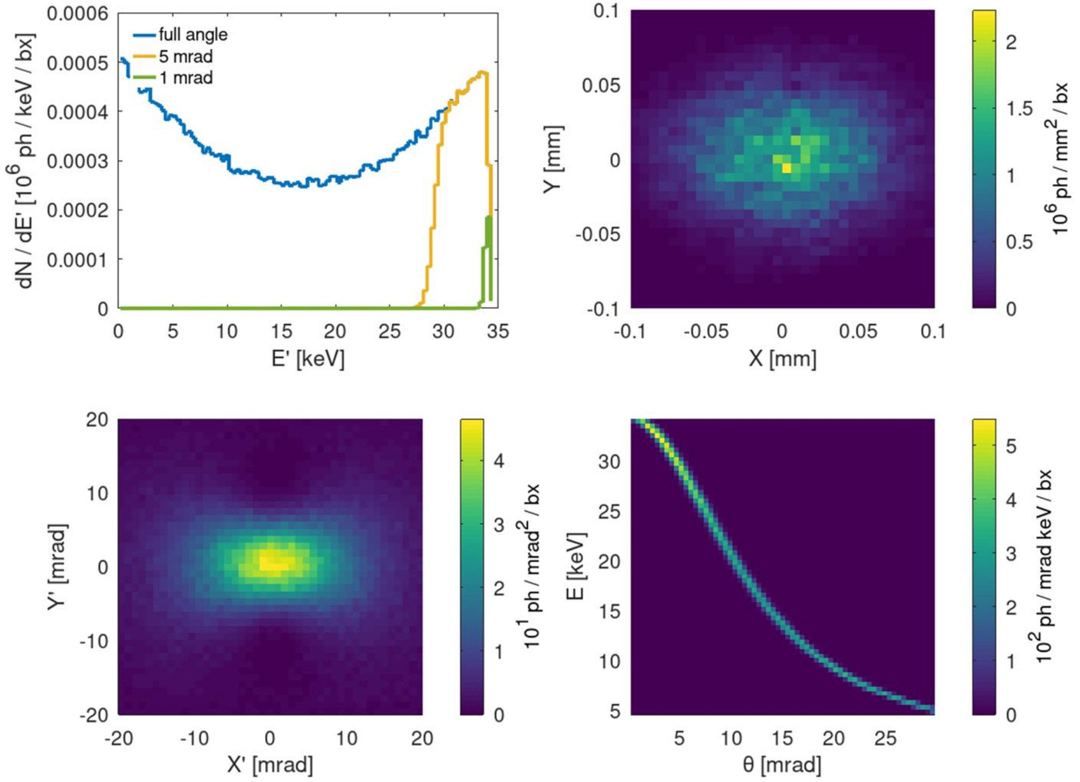

BriXSino: RF-Track

- RF-Track, developed by Andrea Latina [1], was used to simulate ICS sources at the laser and electron beam interaction point (IP).
- Pictured are RF-Track and CAIN simulation results for BriXSino.
- RF-track achieved a much shorter runtime than CAIN.

Parameter	Unit	CAIN	RF-Track	Analytic
Nb. of simulated electrons		10^4	10^4	-
Nb. of generated photons		158149	129839	-
Runtime	s	3276	0.67	0.05
Total flux per shot		9884	11286	11361
Brilliance		1691	1892	1879

Acknowledgements
Alessandro Variola
Iryna Chaikovska
Illya Drebot

[1] Andrea Latina, "RF-Track Reference Manual", CERN, Geneva, Switzerland, June 2020.
[2] A. Variola, J. Haissinski, A. Loulergue, F. Zomer, (eds). ThomX Technical Design Report. 2014, 164

CAIN: Code benchmark

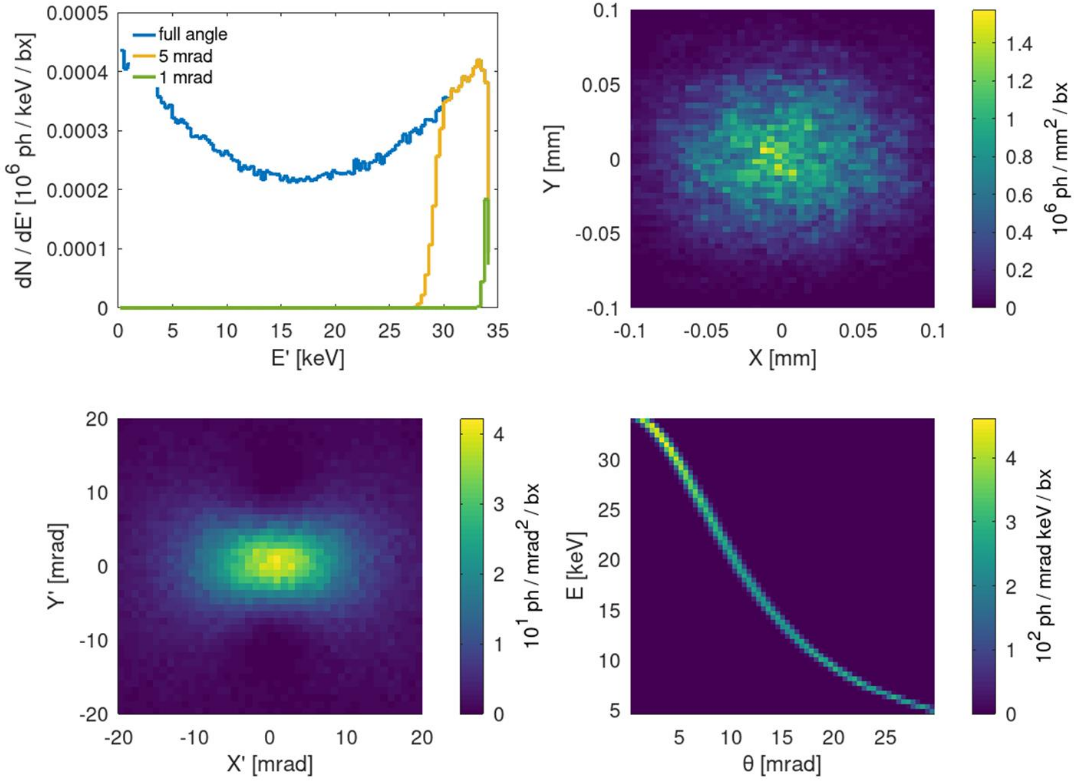

BriXSino: CAIN

- RF-Track, developed by Andrea Latina [1], was used to simulate ICS sources at the laser and electron beam interaction point (IP).
- Pictured are RF-Track and CAIN simulation results for BriXSino.
- RF-track achieved a much shorter runtime than CAIN.

Parameter	Unit	CAIN	RF-Track	Analytic
Nb. of simulated electrons		10^4	10^4	-
Nb. of generated photons		158149	129839	-
Runtime	s	3276	0.67	0.05
Total flux per shot		9884	11286	11361
Brilliance		1691	1892	1879

<u>Acknowledgements</u>

Alessandro Variola

Iryna Chaikovska

Illya Drebot

[1] Andrea Latina, "RF-Track Reference Manual", CERN, Geneva, Switzerland, June 2020.

[2] A. Variola, J. Haissinski, A. Loulergue, F. Zomer, (eds). ThomX Technical Design Report. 2014, 164

XLS: Spot size scans (1.5 mrad cone)

$$\epsilon^N = 0.3 \text{ mm mrad}$$
$$U = 50 \text{ mJ}$$

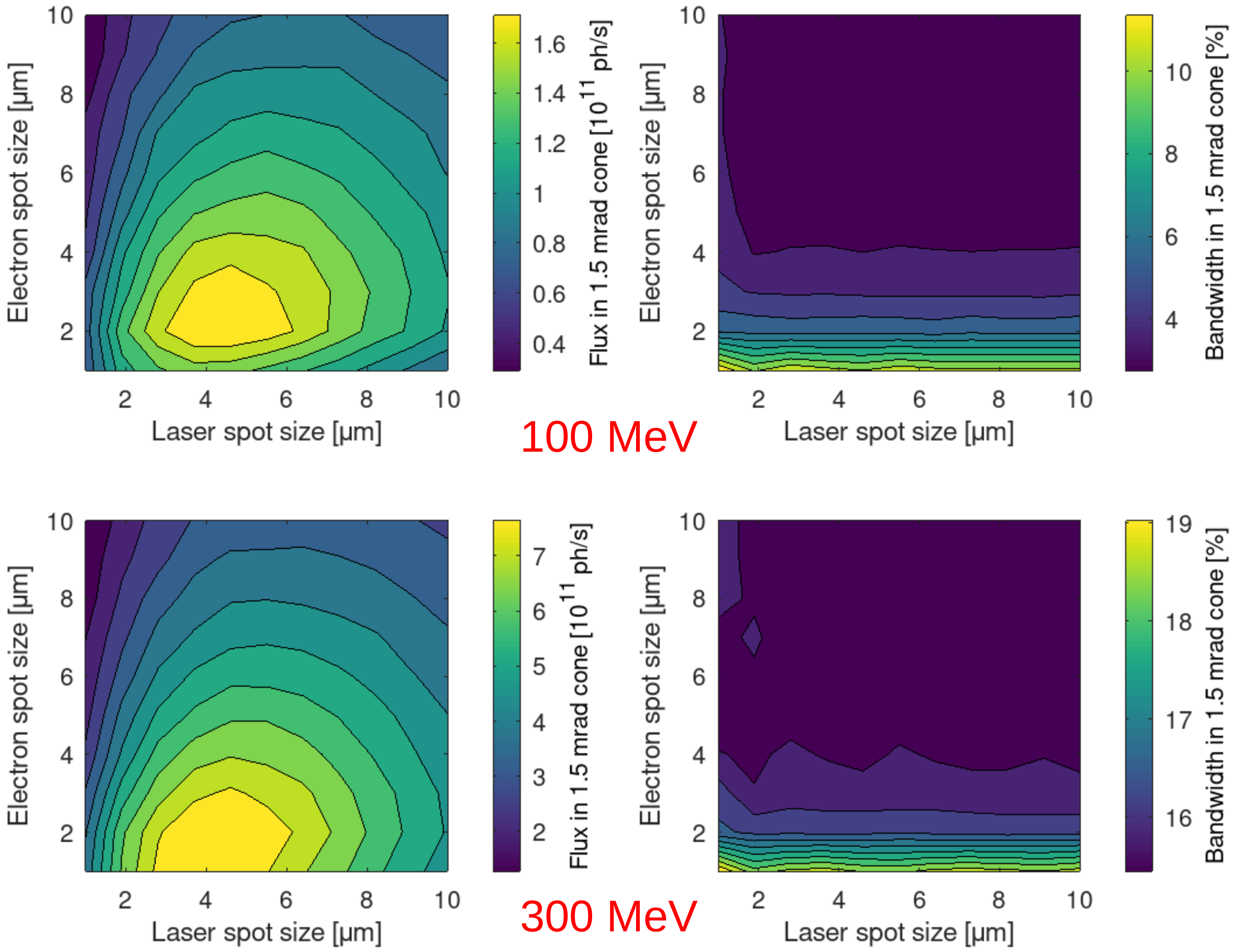

- Dira 1000 laser was used, along with HPCI electron gun
- Applications typically use flux in a 1-2 mrad cone
- Can reduce bandwidth using X-ray monochromators at the expense of flux
- Values for table given for maximum flux

XLS parameter	Unit	100 MeV	300 MeV
Electron spot size	µm	1–4	0.5–3
Laser spot size	µm	3–6	3–6
Flux in 1.5 mrad cone	10^{11}ph/s	1.6	7.0
BW in 1.5 mrad cone	%	4–8	16–19

HPCI: Spot size scans (1.5 mrad cone)

$\epsilon^N = 5$ mm mrad
$U = 6600$ mJ

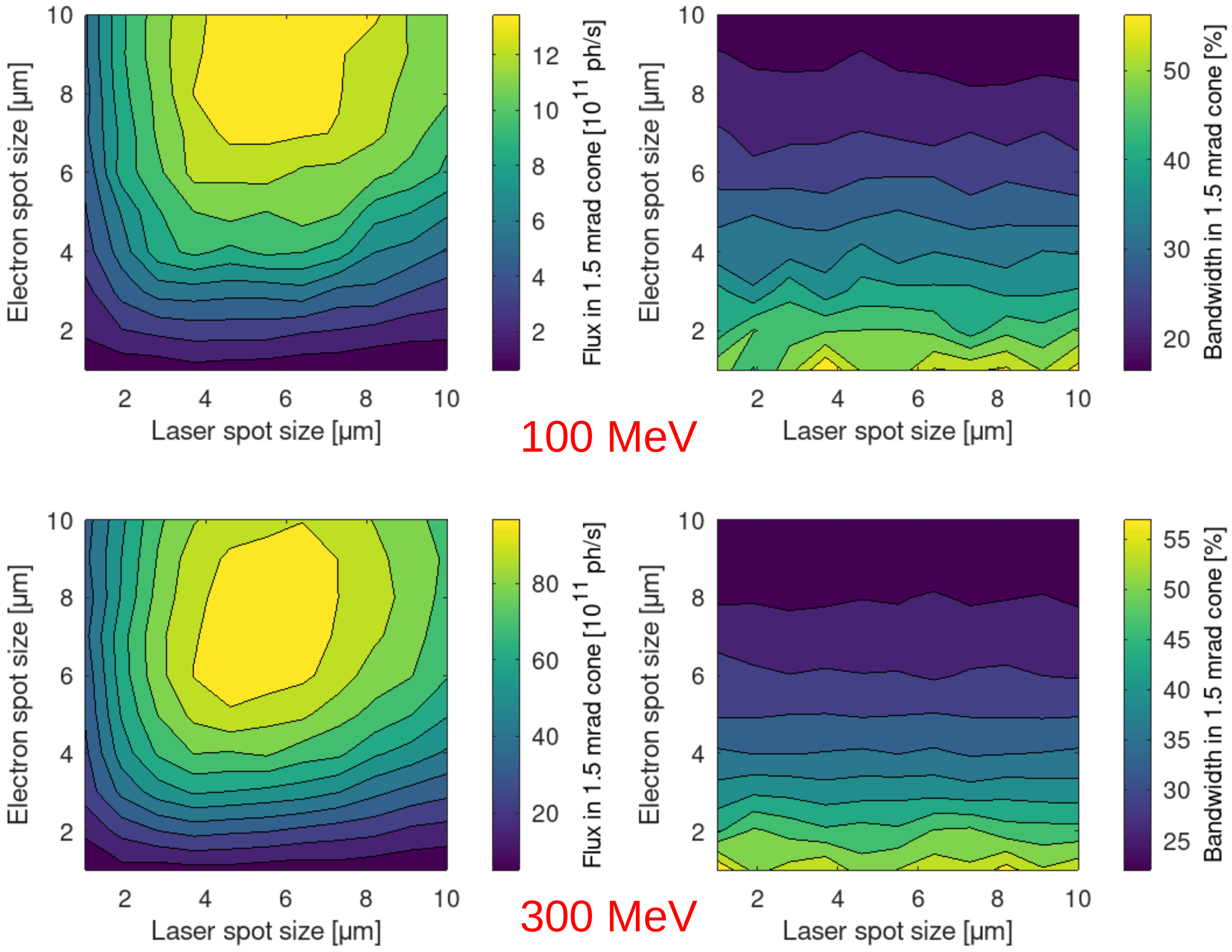

- Dira 1000 laser was used, along with HPCI electron gun
- Applications typically use flux in a 1-2 mrad cone
- Can reduce bandwidth using X-ray monochromators at the expense of flux
- Values for table given for maximum flux

HPCI parameter	Unit	100 MeV	300 MeV
Electron spot size	μm	7–11	5–10
Laser spot size	μm	4–8	3–7
Flux in 1.5 mrad cone	10^{11}ph/s	12	80
BW in 1.5 mrad cone	%	10–20	25–35

Preliminary parameters

Parameter	Symbol	CompactLight		HPCI		Unit
Electron beam energy	E_e	100	300	100	300	MeV
Repetition rate	f	1000		10		Hz
Bunches per train		50		1000		
Collision rate	f_{eff}	50		10		$10^3\,s^{-1}$
Bunch length	σ_z	1		1		ps
Bunch charge	Q	200		300		pC
Bunch spacing		5		1/3		ns
Normalised emittance	$\epsilon^N_{x,y}$	0.3		5		mm mrad
Electron IP spot size	σ_e	1–4	0.5–3.0	7–11	5–10	µm
Laser pulse energy	E_p	50		6.6×10^3		mJ
Pulse length	τ	0.6		0.6		ps
Wavelength	λ	1000		1000		nm
Laser spot size	σ_{laser}	3–6	3–6	4–8	3–7	µm
Total flux	$\mathcal{F}$	1.8×10^{12}	1.8×10^{12}	5.0×10^{13}	6.0×10^{13}	ph/s
Flux in 1.5 mrad	$\mathcal{F}_{1.5\text{ mrad}}$	1.6×10^{11}	7.0×10^{11}	8.0×10^{12}	8.0×10^{12}	ph/s
Average brilliance	$\mathcal{B}$	3.0×10^{13}	2.5×10^{14}	0.3×10^{13}	3.0×10^{13}	(1)
Bandwidth in 1.5 mrad	$BW_{1.5\text{ mrad}}$	4–8	16–19	10–20	25–35	%

(1) ph/(s mm^2 mrad^2 0.1%BW)

- Optimal electron and laser parameters were derived for flux maximization
- Novel ICS sources would benefit from injectors developed at CompactLight and HPCI

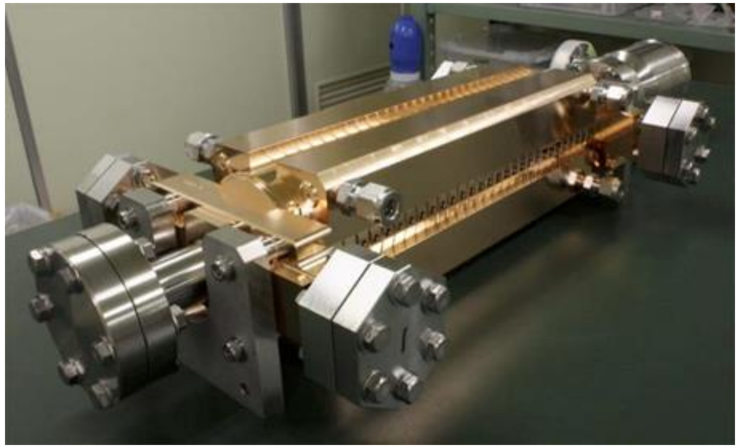

Preliminary parameters

Parameter	Symbol	CompactLight		HPCI		Unit
Electron beam energy	E_e	100	300	100	300	MeV
Repetition rate	f	1000		10		Hz
Bunches per train		50		1000		
Collision rate	f_{eff}	50		10		10^3 s^{-1}
Bunch length	σ_z	1		1		ps
Bunch charge	Q	200		300		pC
Bunch spacing		5		1/3		ns
Normalised emittance	$\epsilon^N_{x,y}$	0.3		5		mm mrad
Electron IP spot size	σ_e	1–4	0.5–3.0	7–11	5–10	µm
Laser pulse energy	E_p	50		6.6×10^3		mJ
Pulse length	τ	0.6		0.6		ps
Wavelength	λ	1000		1000		nm
Laser spot size	σ_{laser}	3–6	3–6	4–8	3–7	µm
Total flux	$\mathcal{F}$	1.8×10^{12}	1.8×10^{12}	5.0×10^{13}	6.0×10^{13}	ph/s
Flux in 1.5 mrad	$\mathcal{F}_{1.5\ \text{mrad}}$	1.6×10^{11}	7.0×10^{11}	8.0×10^{12}	8.0×10^{12}	ph/s
Average brilliance	$\mathcal{B}$	3.0×10^{13}	2.5×10^{14}	0.3×10^{13}	3.0×10^{13}	(1)
Bandwidth in 1.5 mrad	$\text{BW}_{1.5\ \text{mrad}}$	4–8	16–19	10–20	25–35	%

(1) ph/(s mm^2 mrad^2 0.1%BW)

Final focus optimisation

Fabry-Perot cavity geometry

More realistic expectations for flux

HPCI: laser beam offset

- Investigated the change of flux in a 1.5 mrad cone given an offset of the laser in transverse (x, y) or longitudinal directions.
- Values shown for ideal IP parameters

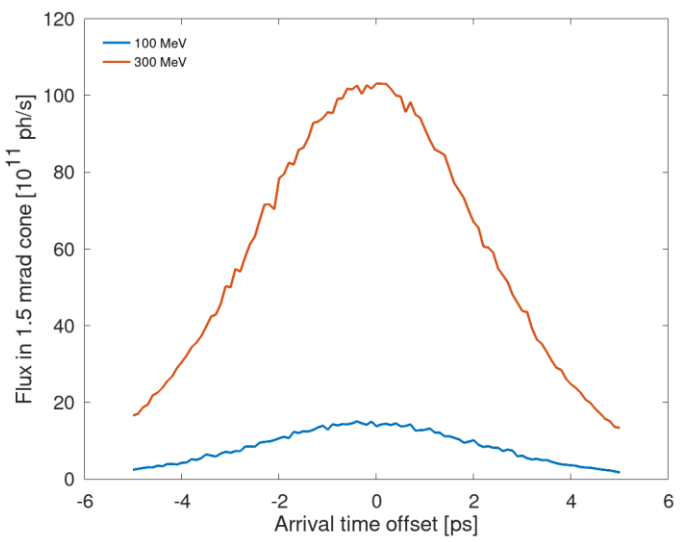

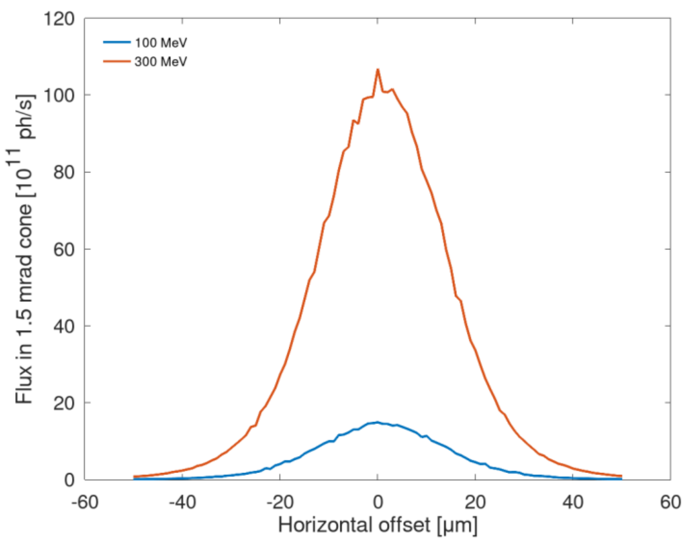

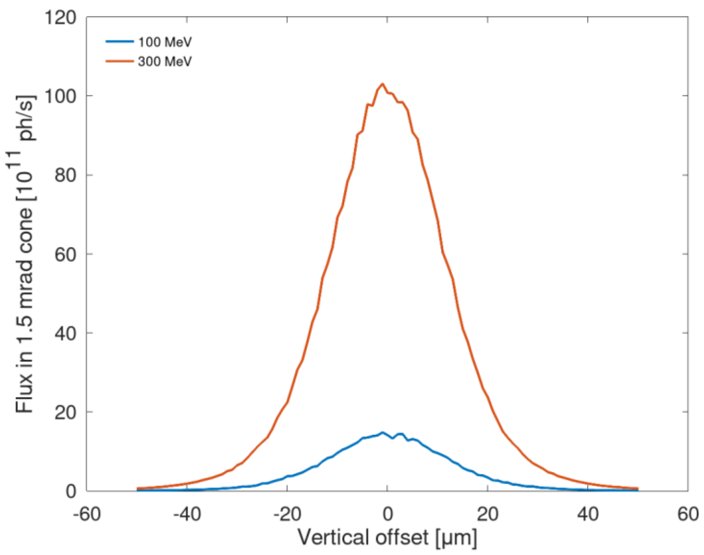

XLS: laser beam offset

- Investigated the change of flux in a 1.5 mrad cone given an offset of the laser in transverse (x, y) or longitudinal directions.
- Values shown for ideal IP parameters

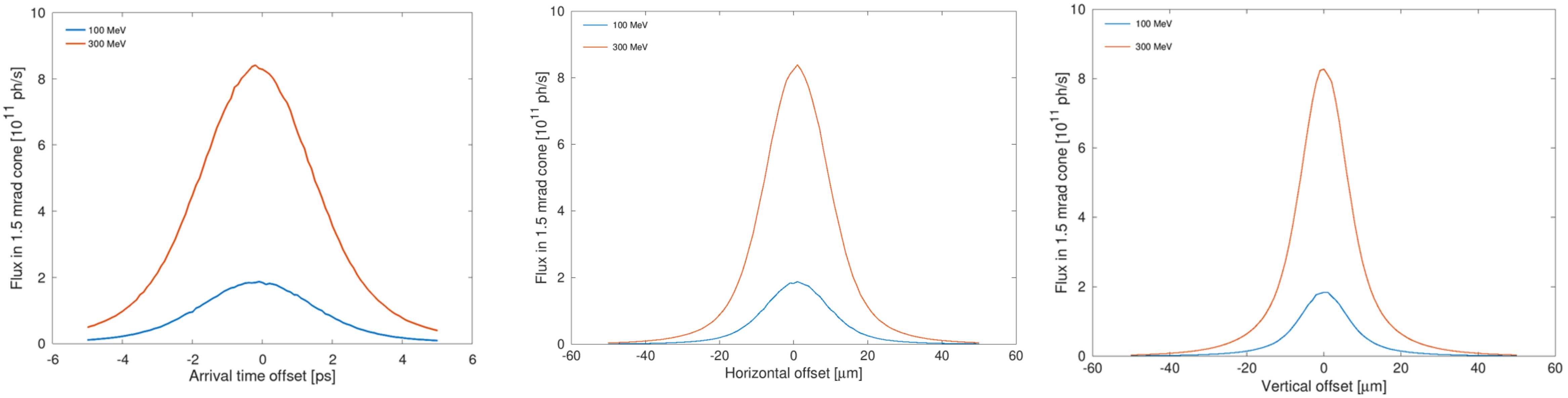

HPCI: laser beam angle offset

- Investigated the change in flux in 1.5 mrad cone given an offset of the laser in pitch (around x-axis) or yaw (around y-axis).
- Asymmetry of yaw plot due to 2° crossing angle.
- Yaw plot has peak larger than other offset plots, since for a misalignment equal to the crossing angle the beams will collide head-on instead and generate the maximum flux.
- Values shown for ideal IP parameters

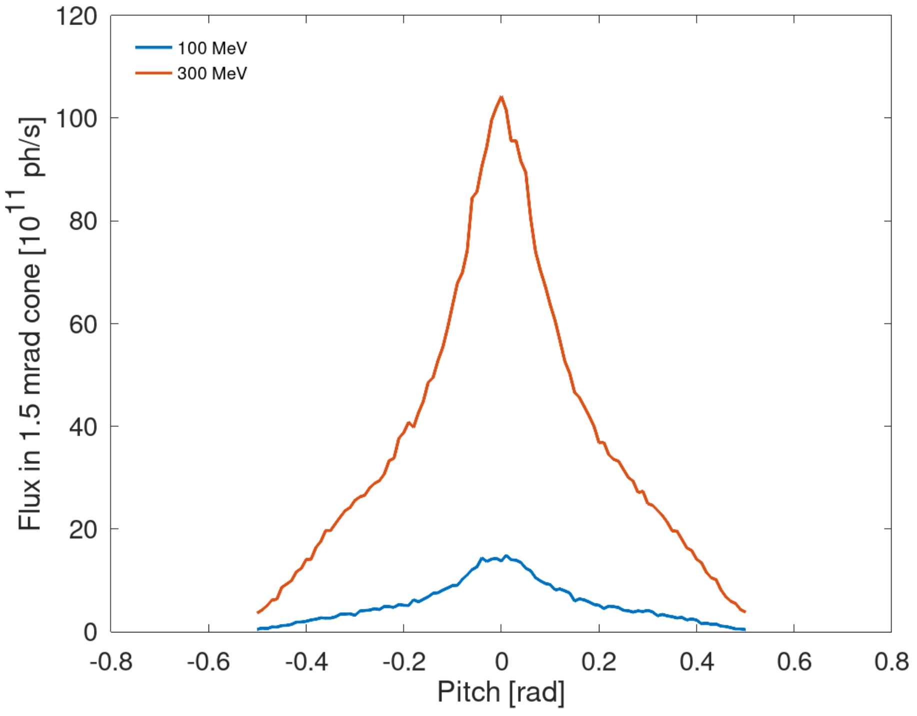

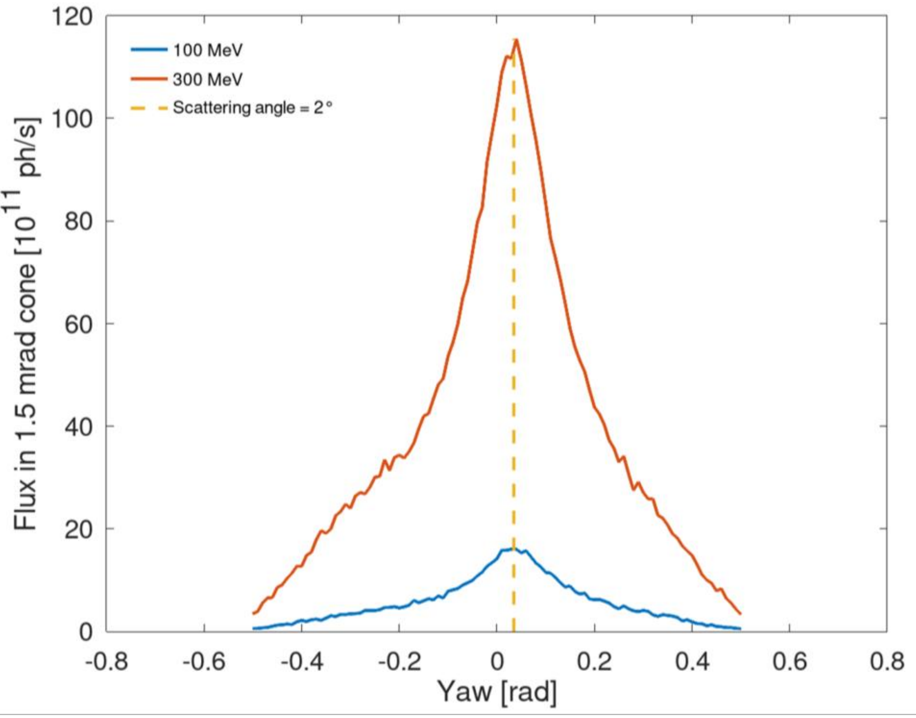

XLS: laser beam angle offset

- Investigated the change in flux in 1.5 mrad cone given an offset of the laser in pitch (around x-axis) or yaw (around y-axis).
- Asymmetry of yaw plot due to 2° crossing angle.
- Yaw plot has peak larger than other offset plots, since for a misalignment equal to the crossing angle the beams will collide head-on instead and generate the maximum flux.
- Values shown for ideal IP parameters

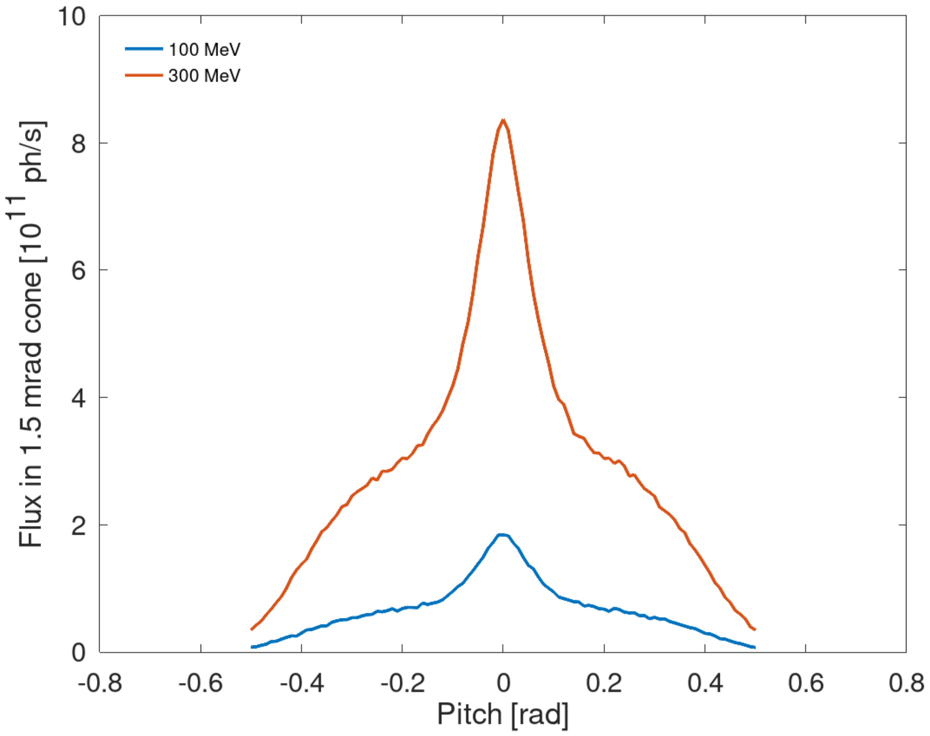

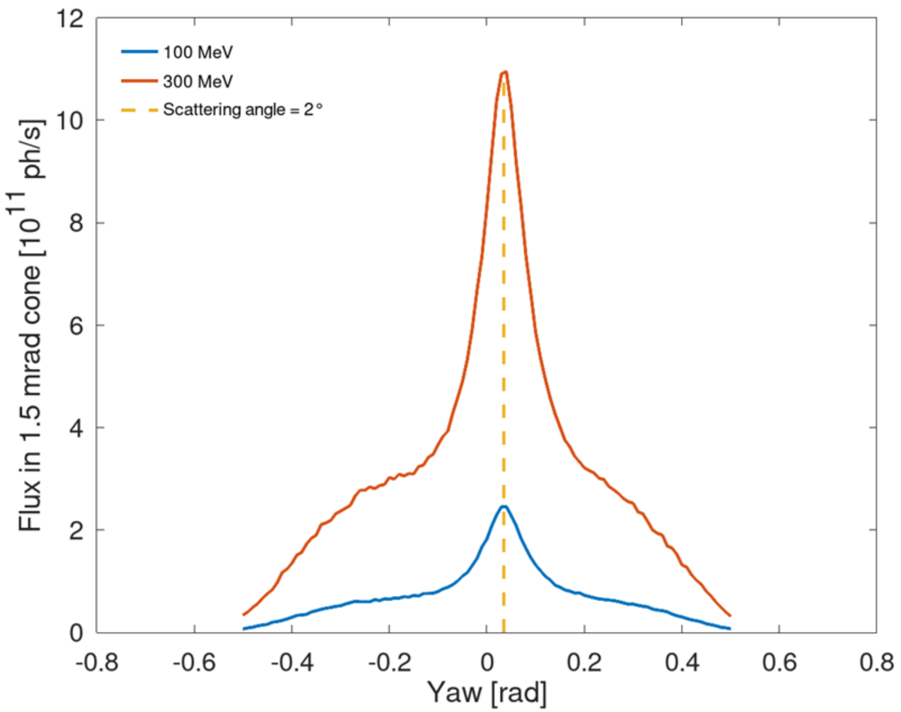

Summary table of offset ranges

- Offset value ranges were computed given a 5% difference to the non-offset flux in 1.5 mrad cone.
- Acceptable offsets range from 1 to 5 μm and 18 to 30 mrad.

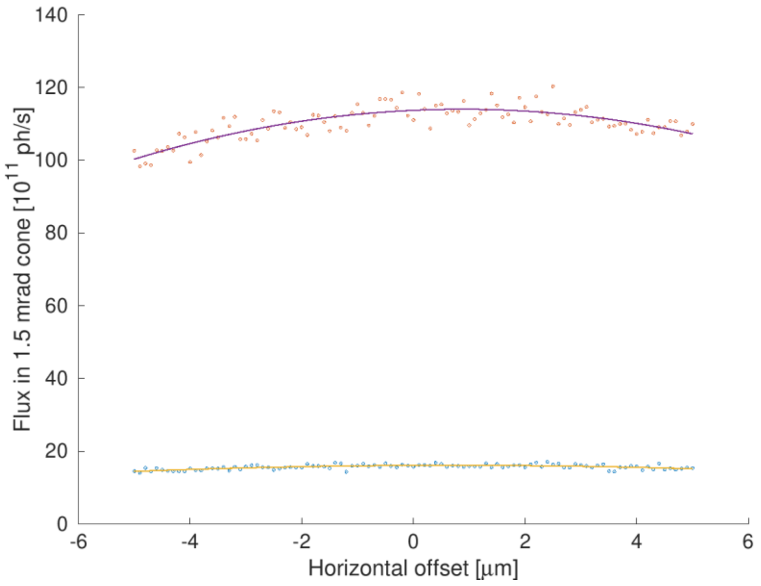

Offset	XLS						HPCI						Unit
	100 MeV			300 MeV			100 MeV			300 MeV			
	Min	Max	Error	Min	Max	Error	Min	Max	Error	Min	Max	Error	
Horizontal	−1.91	2.01	0.10	−1.83	2.06	0.05	−3.06	4.29	0.14	−3.09	4.30	0.09	μm
Vertical	−2.08	2.09	0.02	−2.03	2.06	0.01	−3.51	3.52	0.15	−3.51	3.53	0.05	μm
Arrival time	−0.72	0.40	0.01	−0.71	0.40	0.01	−0.95	0.69	0.02	−0.97	0.61	0.01	ps
Pitch	−18.59	18.49	0.14	−18.44	18.34	0.38	−26.98	27.22	1,37	−26.73	26.49	0.38	mrad
Yaw	−3.58	73.90	0.07	−3.50	73.76	0.09	−7.29	78.29	0.06	−7.49	76.54	0.17	mrad

- Error was calculated as the error on the average of estimates from 3 runs.

XLS: Small final focus design

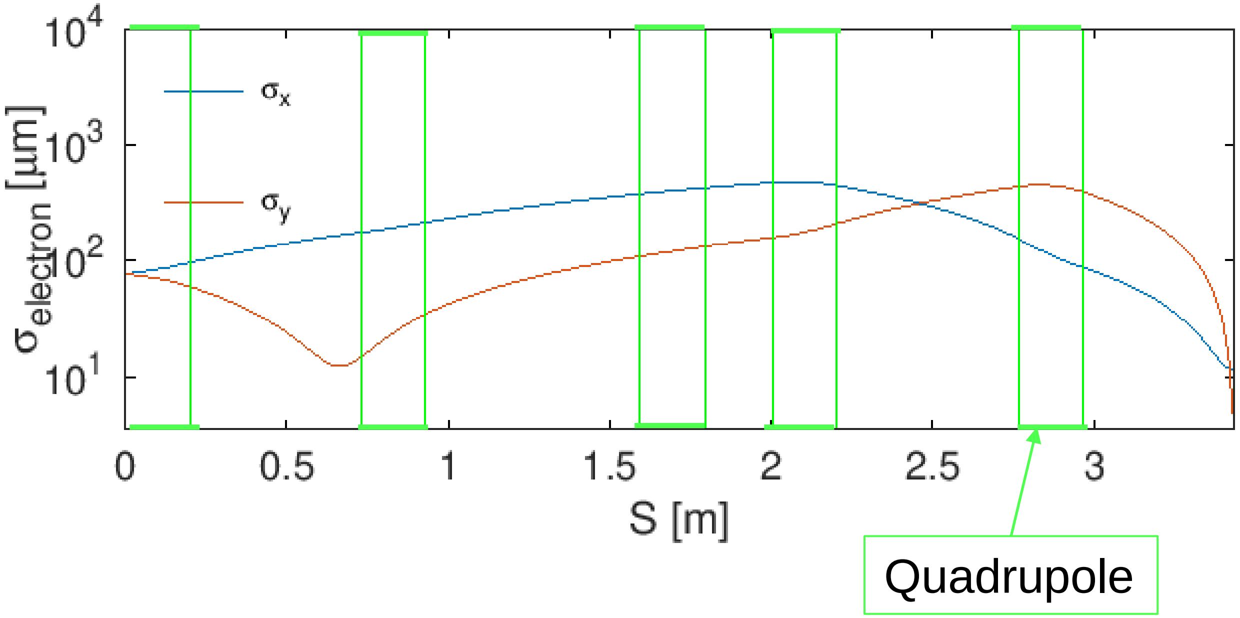

- To determine realistic values for the electron spot size at the IP, an optimisation of the final focus was considered.
- The simplex method for optimisation was used

$$M = 100 \times (\sigma_{x,y}/\sigma_{\text{target}} - 1)^2 + \sigma^2_{x',y'} + 50 \times (\sum \sigma_{\text{Qi}})^2$$

- Free parameters:
  1. Number of Quadrupoles
  2. Quadrupole strength
  3. Distance between Quadrupoles ($L_{\text{Quadrupole}} = 0.2$ m)
  4. $\beta_{x,y}$ at final focus entrance
  5. $\alpha_{x,y}$ at final focus entrance

Parameter	XLS	Unit
σ_x	3.51	μm
σ_y	8.51	μm
σ_{target}	2.5	μm
$\sigma_{x'}$	0.45	mrad
$\sigma_{y'}$	0.24	mrad
Total length	3.70	m
β_x^*	8	mm
β_y^*	36	mm
L*	0.3	m

	G	Unit
1	1.37	Tm^{-1}
2	−1.96	Tm^{-1}
3	1.50	Tm^{-1}
4	−5.32	Tm^{-1}
5	−7.56	Tm^{-1}

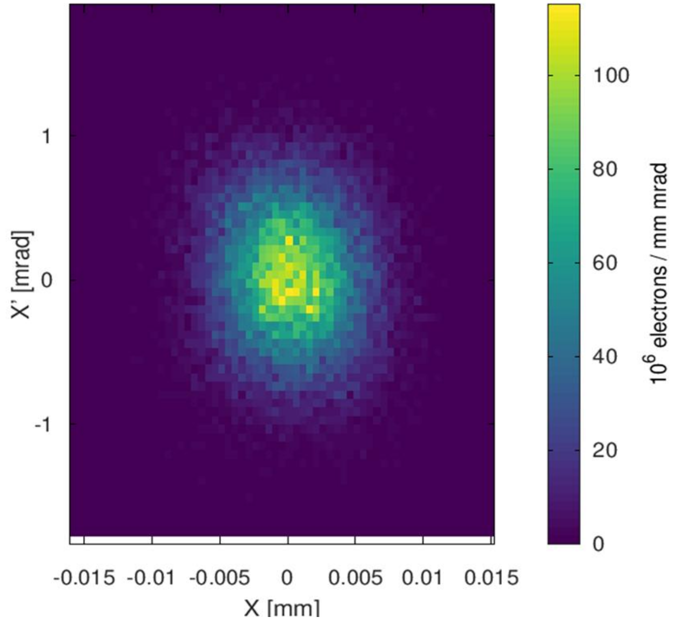

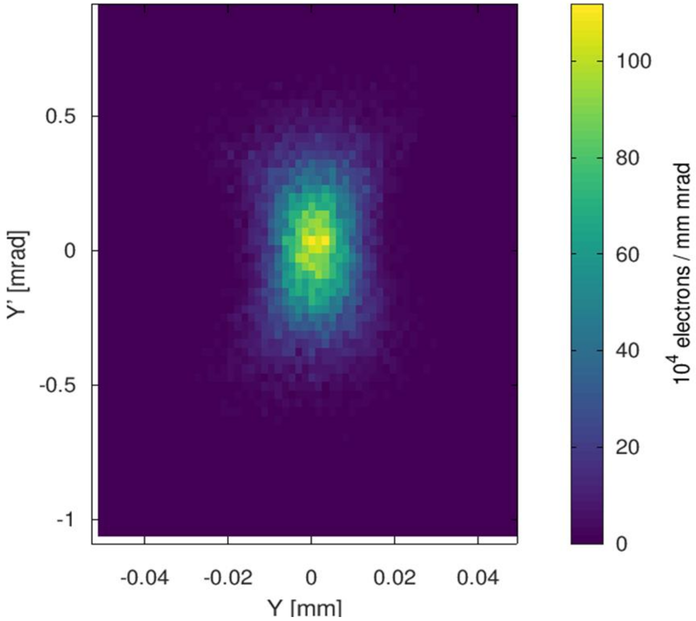

HPCI: Small final focus design

- To determine realistic values for the electron spot size at the IP, an optimisation of the final focus was considered.
- The simplex method for optimisation was used

$$M = 100 \times (\sigma_{x,y}/\sigma_{\text{target}} - 1)^2 + \sigma^2_{x',y'} + 50 \times (\sum \sigma_{\text{Qi}})^2$$

- Free parameters:
  1. Number of Quadrupoles
  2. Quadrupole strength
  3. Distance between Quadrupoles ($L_{\text{Quadrupole}} = 0.2$ m)
  4. $\beta_{x,y}$ at final focus entrance
  5. $\alpha_{x,y}$ at final focus entrance

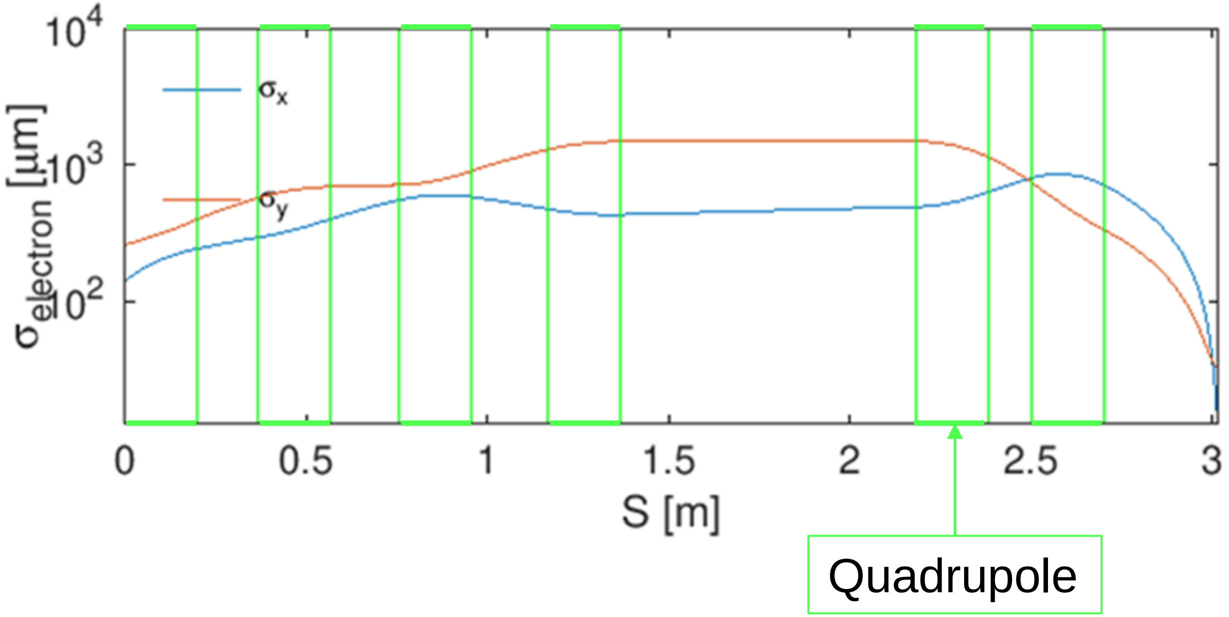

Parameter	HPCI	Unit
σ_x	12.85	μm
σ_y	33.57	μm
σ_{target}	8.00	μm
$\sigma_{x'}$	2.27	mrad
$\sigma_{y'}$	1.07	mrad
Total length	3.02	m
β^*_x	5.7	mm
β^*_y	31.5	mm
L*	0.3	m

	G	Unit
1	-3.38	Tm^{-1}
2	2.37	Tm^{-1}
3	-3.70	Tm^{-1}
4	2.17	Tm^{-1}
5	4.02	Tm^{-1}
6	-7.44	Tm^{-1}

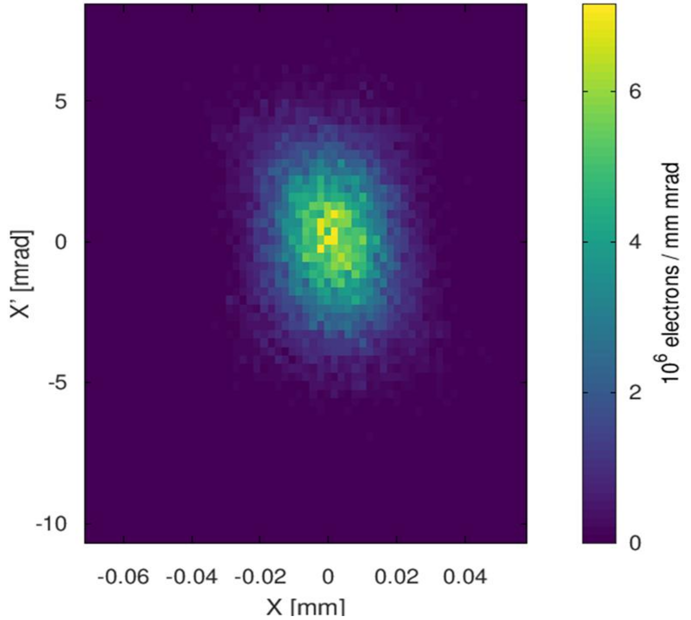

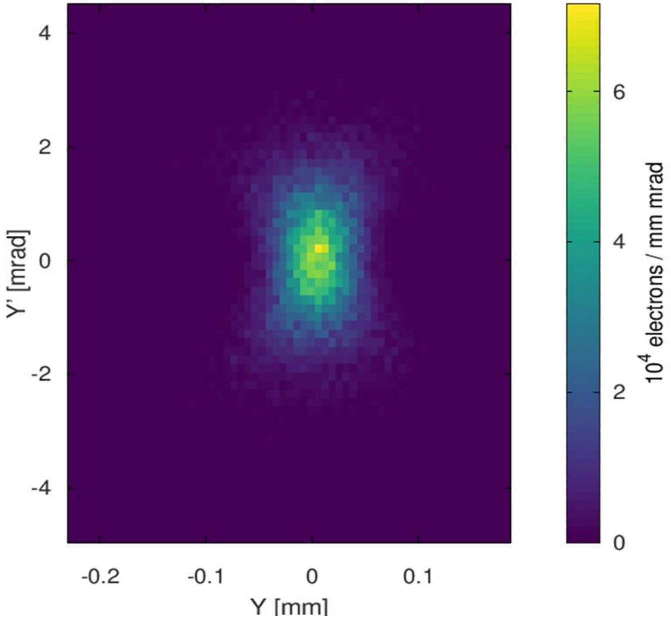

HPCI: Small final focus design
No energy spread

- To determine realistic values for the electron spot size at the IP, an optimisation of the final focus was considered.
- The simplex method for optimisation was used

$$M = 100 \times (\sigma_{x,y}/\sigma_{\text{target}} - 1)^2 + \sigma^2_{x',y'} + 50 \times (\sum \sigma_{\text{Qi}})^2$$

- Free parameters:
  1. Number of Quadrupoles
  2. Quadrupole strength
  3. Distance between Quadrupoles ($L_{\text{Quadrupole}} = 0.2$ m)
  4. $\beta_{x,y}$ at final focus entrance
  5. $\alpha_{x,y}$ at final focus entrance

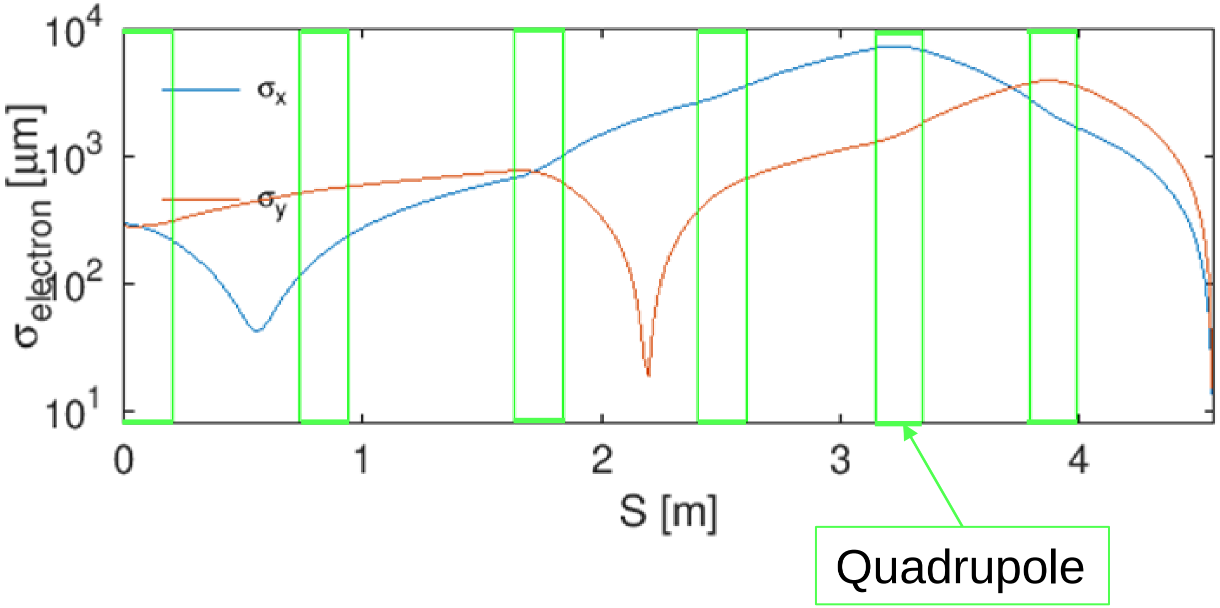

Parameter	HPCI	Unit
σ_x	8.70	μm
σ_y	7.96	μm
σ_{target}	8.00	μm
$\sigma_{x'}$	2.91	mrad
$\sigma_{y'}$	6.19	mrad
Total length	4.56	m
β^*_x	3.00	mm
β^*_y	2.48	mm
L*	0.57	m

	G	Unit
1	−2.76	Tm^{-1}
2	0.33	Tm^{-1}
3	4.64	Tm^{-1}
4	1.91	Tm^{-1}
5	−3.55	Tm^{-1}
6	4.60	Tm^{-1}

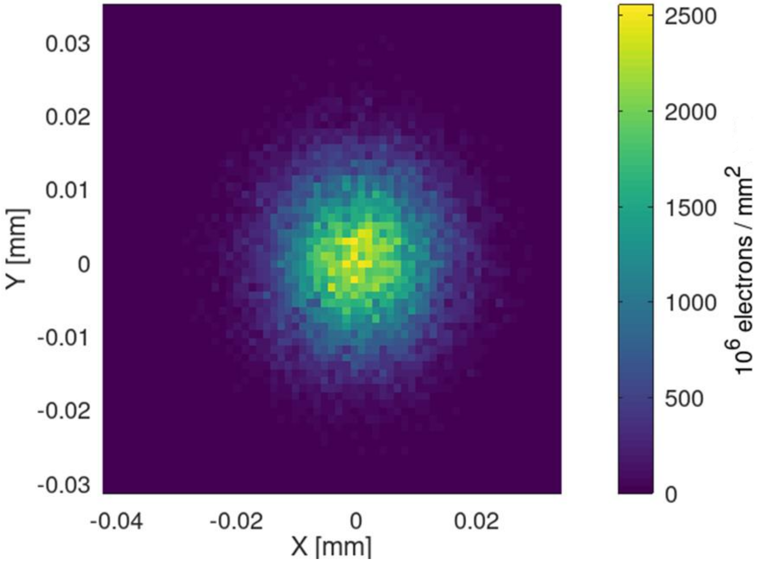

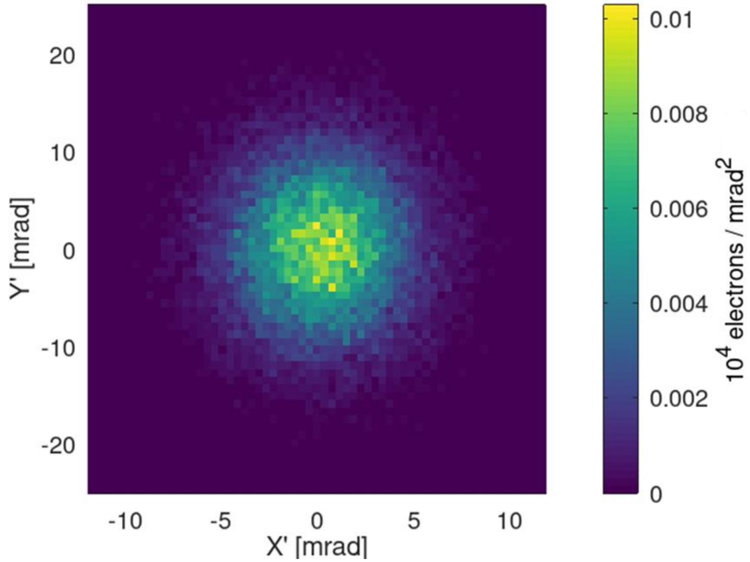

Laser: Preliminary considerations

- A laser similar to TRUMPF's 1 kW Dira 1000 was considered [1].

XLS

- 1 kW and f = 1 kHz → 1 J/pulse, 50 bunches/pulse → E_p = 20 mJ
- Bunch spacing = 5 ns → 200 MHz enhancement cavity

HPCI

- 1 kW and f = 10 Hz → 100 J/pulse, 1,000 bunches/pulse → E_p = 100 mJ
- Bunch spacing = 1/3 ns → 3 GHz enhancement cavity

Enhancement cavities could be used

- In CW for XLS, given a bunch spacing of 5 ns → **E_p = 50 mJ**
- In burst mode for HPCI, given a bunch spacing of 1/3 ns → **E_p = 6.6 J**

Parameter	Quantity	Units
Laser power	1000	W
Pulse length, τ	0.6	ps
Wavelength, λ	1000	nm

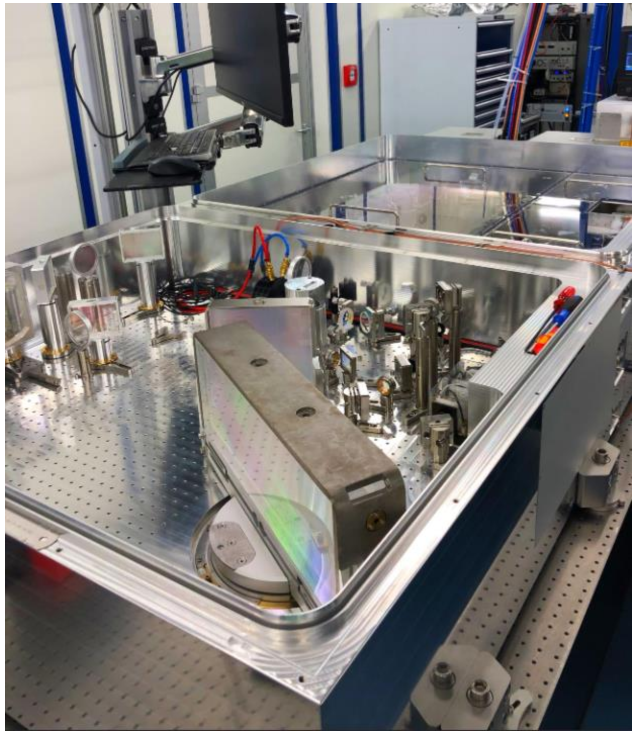

Acknowledgements
Eduardo Granados

➢ **HPCI benefits from Fabry-Perot cavities operated in burst mode**

[1] T. Metzger (November 6 2019), Ultrafast Thin-Disk Amplifiers, Talk S55.

Fabry-Pérot resonator

Acknowledgements
Aurélien Martens

- Fabry-Pérot cavities can greatly increase the available laser pulse energy, which linearly depends on the ICS photon flux.
- **Burst mode operation** prevents mirror coating thermal load by reducing the lower average power inside the cavity.
- The input laser beam repetition rate is matched by the cavity roundtrip length. A subharmonic of the repetition rate can also be considered.
- A burst mode Fabry-Pérot cavity was optimised for the **HPCI**-based ICS source. **XLS** required a low laser repetition rate → more suitable for a Fabry-Perot cavity operated in continuous mode
- The crossing angle α, was chosen to avoid collision of the electron beam with M3/M4. The laser pulse energy was set in correspondence with the maximum fluence $\mathcal{F}$.

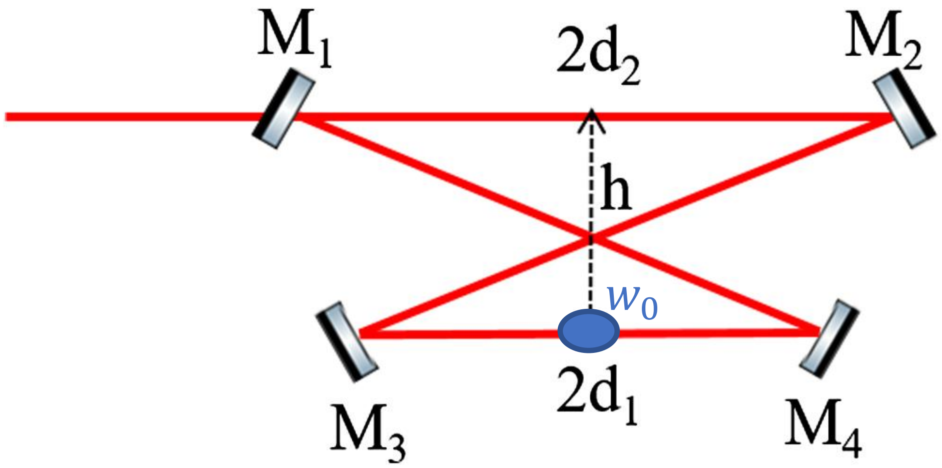

PHYSICAL REVIEW ACCELERATORS AND BEAMS **21,** 121601 (2018)

Optimization of a Fabry-Perot cavity operated in burst mode for Compton scattering experiments

Pierre Favier, Loïc Amoudry, Kevin Cassou, Ronic Chiche, Kevin Dupraz, Aurélien Martens,*
Daniele Nutarelli, Viktor Soskov, and Fabian Zomer
LAL, Univ. Paris-Sud, CNRS/IN2P3, Université Paris-Saclay, 91898 Orsay, France

Antoine Courjaud
Amplitude Systèmes, 11, Avenue de Canteranne, Cité de la Photonique, 33600 Pessac, France

Luca Serafini
INFN-MI, Via Celoria 16, 20133 Milano, Italy

Free parameter	Symbol	Constrain
Spherical mirrors spacing	d_1	$[0, L_{RT}/4]$
Planar mirrors spacing	d_2	
Cavity height	h	
Radius of curvature	R	
Mirror diameter	Φ	$h - \Phi > h\lvert d_1 - d_2\rvert/(d_1 + d_2)$ $d_1 \tan\alpha > \Phi/2$
Roundtrip length	L_{RT}	$n \times c/(2f_{\text{rep}}), n \in \mathbb{Z}$
Laser pulse energy	U	$U < \mathcal{F}_{\max}\pi w_s w_t/2$
Cavity stability		$Tr(M_t) < 2$ $Tr(M_s) < 2$

ABCD matrices

- To compute the laser beam size across the Fabry-Pérot cavity, ray tracing calculations were done using **ABCD matrix** formalism.
- ABCD matrices allow for a fast method to derive parameters describing **Gaussian beams** (lasers or electrons).
- The final ABCD matrix, corresponding to either the sagittal (M_s) or tangential (M_t) waist size, was also used to derive **stability conditions** ($\mathrm{Tr}(M) < 2$)

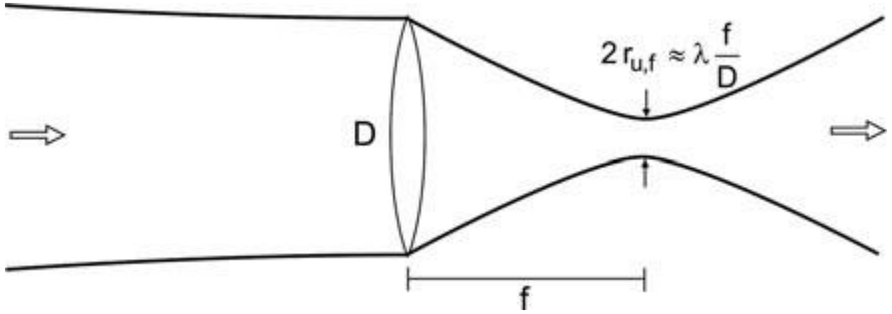

Description	Matrix
Propagation in free space	$\begin{pmatrix} 1 & L \\ 0 & 1 \end{pmatrix}$
Thin lens with f focus length	$\begin{pmatrix} 1 & 0 \\ -\frac{1}{f} & 1 \end{pmatrix}$
Spherical mirror of curvature R	$\begin{pmatrix} 1 & 0 \\ -\frac{2}{R} & 1 \end{pmatrix}$

Familiar?

$$\begin{pmatrix} A & B \\ C & D \end{pmatrix} = \begin{pmatrix} 1 & d_1 \\ 0 & 1 \end{pmatrix} \begin{pmatrix} 1 & 0 \\ -2/(R \times \cos(\theta)) & 1 \end{pmatrix} \begin{pmatrix} 1 & l_{\mathrm{cross}} \\ 0 & 1 \end{pmatrix} \begin{pmatrix} 1 & 0 \\ 0 & 1 \end{pmatrix} \begin{pmatrix} 1 & 2d_2 \\ 0 & 1 \end{pmatrix} \begin{pmatrix} 1 & 0 \\ 0 & 1 \end{pmatrix} \begin{pmatrix} 1 & l_{\mathrm{cross}} \\ 0 & 1 \end{pmatrix} \begin{pmatrix} 1 & 0 \\ -2/(R \times \cos(\theta)) & 1 \end{pmatrix} \begin{pmatrix} 1 & d_1 \\ 0 & 1 \end{pmatrix}$$

STAR: Monte Carlo optimisation

- Marten's paper implemented a Monte Carlo-based optimisation of the Fabry-Pérot cavity geometry. → **results from paper were reproduced (*).**
- Monte Carlo optimisation provided many possible cavity geometries → choose set-up with largest flux.
- However, Monte Carlo methods do not guarantee that the solution for the largest flux is found.

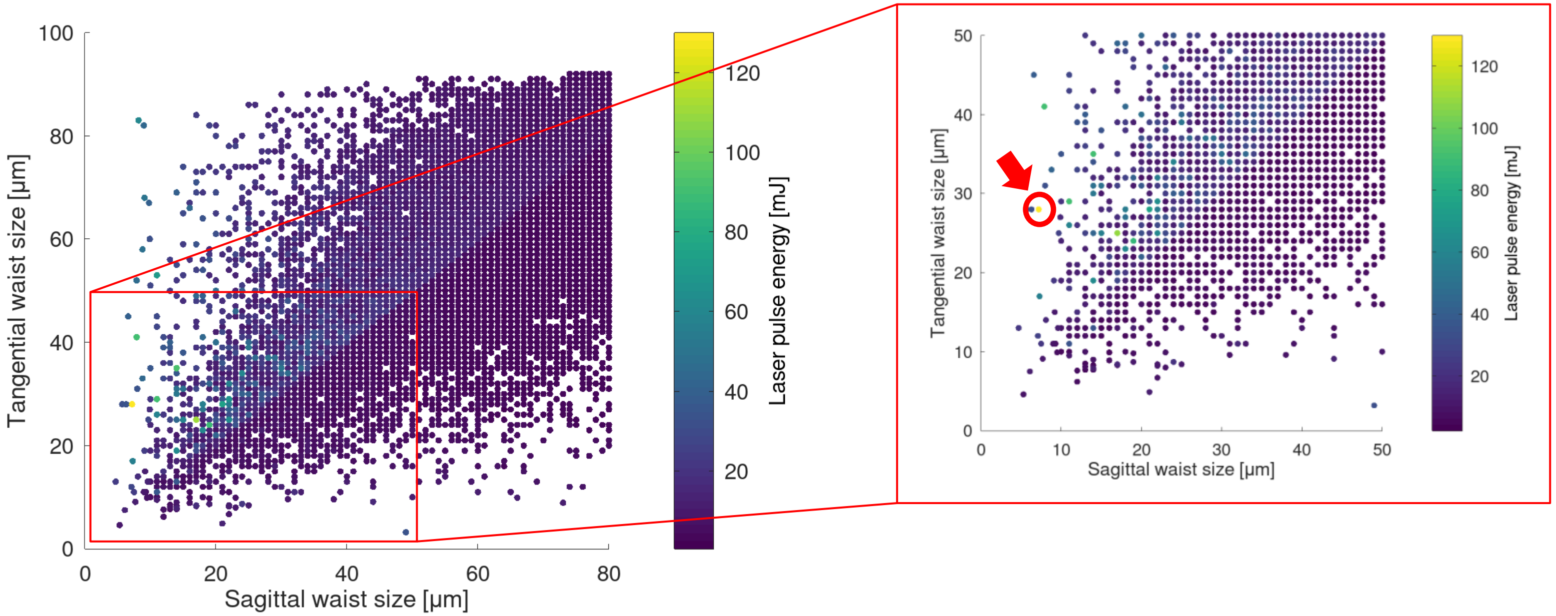

(*)

Method	L_{RT} [m]	$2d_1$ [cm]	$2d_2$ [cm]	h [cm]	α [degree]	R [cm]	$\bar{\Phi}$ [cm]	U_{max} [mJ]	$w_{0\mathrm{s}}/w_{0\mathrm{t}}$ [μm/μm]	$\mathcal{F}$ [ph/s]
Monte Carlo	1.2	24.4	35.5	1.66	4.1	24.4	1.35	130	14/26	6.9×10^{11}
Monte Carlo	0.3	6.6	8.31	0.77	6.0	6.6	0.587	22	9/19	3.6×10^{11}

STAR: Simplex optimisation

- The simplex algorithm is a fast method to arrive at a minimum of a merit function. In comparison with Monte Carlo, the script runtime was greatly reduced, and a definite maximum was reached for the photon flux.
- Bias was avoided for the merit function; weights were chosen to prioritize parameter constraints and allow for sensible solutions.
- Practical constraints were set for the laser pulse energy and waist sizes:
  - $5\ \mathrm{mJ} < U < 150\ \mathrm{mJ}$
  - $\sigma_{\mathrm{electron}} < w_0 \ll \Phi$

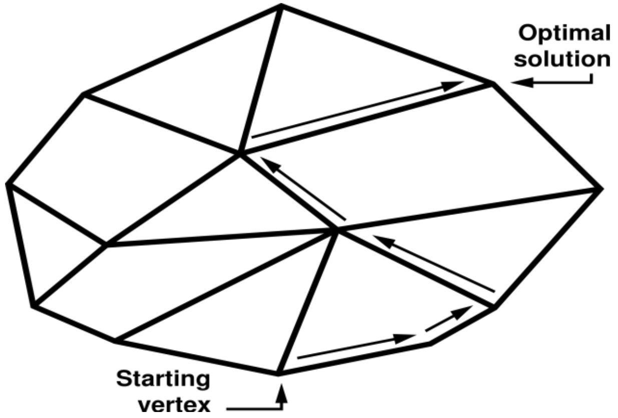

- **Minimised:**
  - Laser waist size, w_{0s}/w_{0t}
  - Crossing angle, α
- **Maximised:**
  - Laser pulse energy, U
  - Flux, $\mathcal{F}$

$$M = -U^2 + 100 \times \{(w_{0s} < 30)^2 + (w_{0t} < 30)^2 + (w_{0s} > 5)^2 + (w_{0t} > 5)^2 + (\mathrm{Tr}(M_t) < 2)^2 + (\mathrm{Tr}(M_s) < 2)^2 + (U < 140)^2 + (h - \Phi > h|d_1 - d_2|/(d_1 + d_2))^2\}$$

Method	L_{RT} [m]	$2d_1$ [cm]	$2d_2$ [cm]	h [cm]	α [degree]	R [cm]	Φ [cm]	$U_{\max}$ [mJ]	w_{0s}/w_{0t} [μm/μm]	$\mathcal{F}$ [ph/s]
Monte Carlo	1.2	24.4	35.5	1.66	4.1	24.4	1.35	130	14/26	6.9×10^{11}
Simplex	1.2	24.6	35.3	1.23	2.1	24.6	0.80	140	16/23	1.1×10^{12}
Monte Carlo	0.3	6.6	8.31	0.77	6.0	6.6	0.587	22	9/19	3.6×10^{11}
Simplex	0.3	6.32	8.65	0.59	4.8	6.3	0.500	22	9/16	3.9×10^{11}

Cavity geometry optimisation

Parameter	Symbol	HPCI		Unit
Electron beam energy	E_e	100	300	MeV
Collision rate	f_{eff}	10		10^3 s^{-1}
Bunch length	σ_z	1		ps
Bunch charge	Q	300		pC
Bunch spacing		1/3		ns

- For HPCI, chose L_{RT} = 1.5 m to minimize the crossing angle and maximise the flux.
- L_{RT} = 1.5 m corresponds to a subharmonic of the laser repetition rate.
- Both Monte Carlo and simplex methods were used for cavity optimization.
- XLS' 200 MHz cavity repetition rate was not suitable for burst mode operation → NO cavity optimization

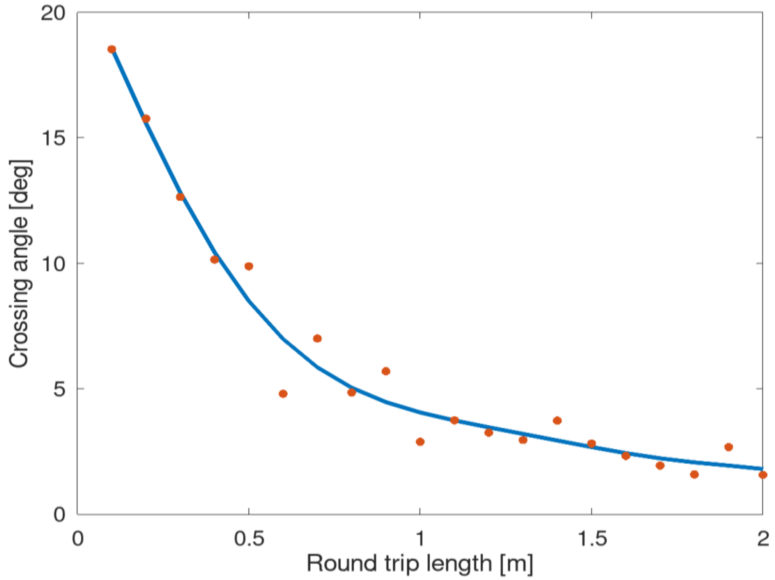

Energy [MeV]	Optimisation method	L_{RT} [m]	$2d_1$ [cm]	$2d_2$ [cm]	h [cm]	α [degree]	R [cm]	Φ [cm]	$U_{\max}$ [mJ]	w_{0s}/w_{0t} [μm/μm]	Flux [ph/s] ideal IP	Flux [ph/s] post-FFS
100	Monte Carlo	1.5	14.157	60.6	3.7	2.86	14.14	0.635	144.83	5.88/19.66	5.76×10^{13}	1.70×10^{13}
100	Simplex	1.5	15.33	51.13	25.30	3.33	14.53	0.685	140	8.54/6.30	1.09×10^{14}	3.21×10^{13}
300	Monte Carlo	1.5	15.8	59.1	2.16	2.4	15.79	0.635	136.02	9.16/16.84	5.71×10^{13}	1.73×10^{13}
300	Simplex	1.5	14.42	52.62	24.44	4.06	13.70	0.786	140	10.0/4.86	1.05×10^{14}	3.18×10^{13}

HPCI: Post final focus and Fabry-Perot cavity optimisation parameters

Parameter	Symbol	HPCI		Unit
Electron beam energy	E_e	100	300	MeV
Electron IP spot size	σ_e	7–11	5–10	µm
		12.9/33.6		
Laser pulse energy	E_p	6.6×10^3		mJ
		13×10^3		
Laser spot size	σ_{laser}	4–8	3–7	µm
		8.5/6.3	10.0/4.9	
Total flux	$\mathcal{F}$	5.0×10^{13}	6.0×10^{13}	ph/s
		3.2×10^{13}		

- The optimisation of the final focus and Fabry-Pérot cavity geometry led to a more realistic estimate for flux.
- The linac structure was considered and adapted to maximise flux.
- XLS could not benefit from the burst mode cavity optimisation.

Conclusions

- Electron beam parameter ranges were determined, based on CompactLight and HPCI injectors
- Laser parameters based on TRUMPF's 1 kW Dira 1000 laser were used.
- Tolerance studies of the laser beam offset were derived. Tolerances depend on requirements set by each application.
- Optimisation of the Fabry-Pérot cavity geometry resulted in flux values of 10^{14} ph/s for HPCI and 10^{12}ph/s XLS, a photon intensity larger than any other existing or commissioned ICS source.
- A small final focus of the electron beam is being designed and optimised. From preliminary results, XLS allowed for smaller beam sizes to be achieved, due to the smaller emittance.
- Potential applications for high energy and high intensity x-rays include FLASH therapy, nuclear waste management, and semiconductor wafer inspection.
- Next steps: complete optimisation of the Fabry-Pérot cavity (effective gain); decide on application and compute the required parameters.

Name	E_{Xray} [keV]	$\mathcal{F}$ [ph/s]	BW [%]	σ_{Xray} (at IP) [μm]	σ_{Xray} (at sample) [mm]	Θ [mrad]
K-edge subtraction	33.7	3×10^{10}	4.5	45×45	62×74	4
Phase contrast imaging	25	2.4×10^{9}	4	39×45	16×16	4
Microbeam radiation therapy	25	10^{13}	3.6	70	4	1.5
FLASH therapy	6,000-10,000 (?)	10^{14} (?)	-	50	17	-
Protein crystallography	7-35	10^{13}	1.4	30	30	2
XRF	6.5-92	3×10^{10}	1-3	20	20 μm	-
Nuclear waste management	1,000-5,000	2.2×10^{13}	0.2	35	-	-
Semiconductor wafer inspection	20	10^{8}	1	-	100 μm	1
HPCI	< 2000	$< 10^{14}$	20–50	> 4	> 4	> 0.5
XLS	< 2000	$< 10^{12}$	1–20	> 10	> 10	> 0.5

Preliminary